Mineralogical Magazine, August 2004, Vol. 68(4), pp. 615–632

Skaergaardite, PdCu, a new platinum-group intermetallic mineral from the Skaergaard intrusion, Greenland

N. S. RUDASHEVSKY[1,*], A. M. MCDONALD[2], L. J. CABRI[3,4], T. F. D. NIELSEN[5], C. J. STANLEY[6], YU. L. KRETZER[1] AND V. N. RUDASHEVSKY[1]

[1] Centre for New Technologies, Svetlanovsky ave. 75-41, St. Petersburg, 195427 Russia
[2] Department of Earth Sciences, Laurentian University, Ramsy Lake Road, Sudbury, Ontario, Canada
[3] Cabri Consulting Inc., 99, Fifth Avenue, Suite 122, Ottawa, Ontario, Canada K1S 5P5
[4] CANMET/MMSL, Ottawa, Canada K1A 0G1
[5] Geological Survey of Denmark and Greenland, Øster Voldgade 10, DK-1350 Copenhagen K, Denmark
[6] The Natural History Museum, Cromwell Road, London SW7 5BD, UK

ABSTRACT

Skaergaardite, PdCu, is a new mineral discovered in the Skaergaard intrusion, Kangerdlugssuaq area, East Greenland. It occurs in a tholeitiic gabbro associated with plagioclase, clinopyroxene, orthopyroxene, ilmenite, titanian magnetite, fayalite and accessory chlorite-group minerals, ferrosaponite, a member of the annite–phlogopite series, hornblende, actinolite, epidote, calcite, ankerite, apatite and baddeleyite. The mineral is found in composite microglobules composed of bornite, chalcocite, digenite, chalcopyrite, with rare cobalt pentlandite, cobaltoan pentlandite, sphalerite, keithconnite, vasilite, zvyagintsevite, (Cu,Pd,Au) and Pt-Fe-Cu-Pd alloys, unnamed $PdCu_3$, (Pd,Cu,Sn), Au_3Cu and PdAuCu. Skaergaardite occurs as droplets, equant grains with rounded outlines, subhedral to euhedral crystals and as irregular grains that vary in size from 2 to 75 μm, averaging 22 μm. It is steel grey with a bronze tint, has a black streak, a metallic lustre and is sectile. Neither cleavage nor fracture was observed. The mineral has a micro-indentation hardness of VHN_{25} = 257. It is isotropic, non-pleochroic and exhibits neither discernible internal reflections nor evidence of twinning. Skaergaardite varies from bright creamy white (associated with bornite and chalcopyrite) to bright white (associated with digenite and chalcocite). Reflectance values in air (and in oil) are: 58.65 (47.4) at 470 nm, 62.6 (51.1) at 546 nm, 64.1 (52.8) at 589 nm and 65.25 (53.95) at 650 nm. The average of 311 electron-microprobe analyses gives: Pd 58.94, Pt 1.12, Au 2.23, Cu 29.84, Fe 3.85, Zn 1.46, Sn 1.08, Te 0.28 and Pb 0.39, total 99.19 wt.%, corresponding to $(Pd_{0.967}Au_{0.020}Pt_{0.010})_{\Sigma 0.997}(Cu_{0.820}Fe_{0.120}Zn_{0.039}Sn_{0.016}Te_{0.004}Pb_{0.003})_{\Sigma 1.002}$. The mineral is cubic, space group $Pm3m$, a = 3.0014(2) Å, V = 27.0378 Å^3, Z = 1. D_{calc} is 10.64 g/cm^3. The six strongest lines in the X-ray powder-diffraction pattern [d in Å(I)(hkl)] are: 2.122(100)(110), 1.5000(20)(200), 1.2254(50)(211), 0.9491(20)(310), 0.8666(10)(222), 0.8021(70)(321). The mineral has the CsCl-type structure. It is believed to be isostructural with wairauite (CoFe), synthetic CuZn (β-brass) and is structurally related to hongshiite (PtCu). Skaergaardite developed from a disordered Pd-Cu-rich metal alloy melt that had exsolved from an earlier Cu-(Fe) sulphide melt. Ordering of Pd and Cu (beginning at $T \approx$ 600ºC) results in development of the CsCl structure from a disordered face-centred cubic structure.

KEYWORDS: skaergaardite, Pd-Cu intermetallic, new mineral species, CsCl-type structure, platinum-group elements, hydroseparation, Skaergaard intrusion, Greenland, Duluth intrusion, Minnesota.

Introduction

SKAERGAARDITE, PdCu, is a new mineral discovered in a drill core taken from the Skaergaard intrusion (N68º09′55″; W31º41′02″),

* E-mail: rudash@online.ru
DOI: 10.1180/0026461046840208

Kangerdlugssuaq area, East Greenland. The mineral was found in sample 90-24, 1057 that was recovered from BQ (diameter = 4 cm) drill core #90-24 taken from the Pd5 level at a depth of between 1057 and 1058 m. It was initially recovered from non-magnetic, heavy-mineral separates from sample 90-24 1057 (initial mass = 0.78 kg) produced using a HS-01 Hydroseparator (Rudashevsky *et al*., 2001, 2002; Cabri, 2004). The process produced 354 skaergaardite particles and skaergaardite-bearing sulphide aggregates of dimensions up to 0.1 mm. It was also subsequently found in two polished thin sections (12 grains). A similar mineral has previously been reported from the Duluth intrusion, Minnesota, (Komppa 1998), and the Rum layered intrusion, Scotland (Power *et al*., 2000).

The name is for the locality. Both the mineral and mineral name were approved by the Commission on New Minerals and Mineral Names, IMA (IMA 2003-049). Holotype material is catalogued in the collections of the Geologisk Museum, Copenhagen (five polished sections: 90-24 1057 45-1, 90-24 1057 45-2, 90-24 1057 125-2, 90-24 1057 125-3; catalogue no GM 2004.66), the Natural History Museum, London (polished section; catalogue no BM 2003,47) and the Canadian Museum of Nature, Ottawa (polished section 90-24 1057 75-1; catalogue no. CMNMC 84396).

Occurrence, origin and associated minerals

The Skaergaard intrusion is an oval-shaped (~10 × 7.5 km), rhythmically layered gabbroic body that was emplaced into a basement of Achaean granitic gneiss and related rocks during the Eocene (Irvine, 1992). It is renowned for its rhythmic layering, extreme compositional differentiation, and igneous structures (Irvine *et al*., 2001) and portions of it have been prospected for noble metals (e.g. the Triple Group, which contains a notable enrichment in both Au and Pd; Andersen *et al*., 1998).

Skaergaardite occurs in a well-preserved, oxide-rich, tholeitic gabbro in what is referred to as the Platinova Reef (Nielsen *et al*., 2003). The gabbro is found in the Triple Group, which constitutes the upper 100 m of the Middle zone in the Layered series of the intrusion. The associated platinum-group element (PGE) and Au mineralization is stratiform in nature. The average Pd concentration over the interval in which skaergaardite was found (1057–1058 m) is 2.8 g/t, with an average combined Pt+Pd+Au of 3.1 g/t (Nielsen *et al*., 2003). The gabbro hosting the mineral is composed of plagioclase (An_{44-49}), clinopyroxene (Mg# = 0.60–0.63), orthopyroxene (Mg# = 0.53–0.49), ilmenite, titanian magnetite, fayalite (Mg# = 0.40–0.50), as the rock-forming minerals, and small amounts of accessory chlorite-group minerals, ferrosaponite, a member of the annite–phlogopite series, hornblende, actinolite, epidote-group minerals, calcite, ankerite, apatite and baddeleyite. Sulphides (predominantly Cu-Fe-bearing) constitute ~0.05 modal% of the platinum-group element-bearing mineralization zone, typically occurring at interstices between Fe-Ti oxides and pyroxene grains (Fig. 1*a*), but also occasionally intergrown with H_2O-bearing silicates (Fig. 1*b*). The H_2O-bearing silicates occur proximal to sulphide and Fe-Ti oxide aggregates, and do not replace rock-forming silicates. It may also be significant that linear exsolution lamellae in composite pyroxene grains (orthopyroxene + clinopyroxene) are noticeably disrupted around inclusions of both sulphides and Fe-Ti oxides (Fig. 1*b*,*c*; Fig. 2*b*).

The sulphide inclusions may be best described as Cu-Fe sulphide aggregates, consisting primarily of bornite along with either chalcocite or digenite, but all in variable ratios. Morphologically, the aggregates can be either irregular in shape (Fig. 1*c*) or have a rounded to droplet-like outline (Fig. 1*d–f*). The latter are typically <0.1 mm in diameter and are more accurately described as microglobules. Frequently, these microglobules exhibit distinct exsolution textures (chalcocite from bornite; Fig. 1*e*,*f*). Additional sulphides observed within the microglobules include chalcopyrite (found in ~3% of the particles studied), cobaltoan pentlandite, cobalt pentlandite and sphalerite. Skaergaardite may be found as inclusions in titanian magnetite (Fig. 2*a*), ilmenite, pyroxenes (Fig. 2*b*,*d*,*e*), and plagioclase (Fig. 2*b*,*f*).

While skaergaardite is the dominant PGM in the environment (representing >90% of the total PGM observed), other PGM and precious-metal-bearing minerals are present (both as inclusions and discrete grains) including: keithconnite, $Pd_{3-x}Te$, (as inclusions in 11 skaergaardite and unnamed $PdAuCu_2$ grains; Fig. 3*b*,*c*), vasilite, $(Pd,Cu)_{16}(S,Te)_7$ (as inclusions in six skaergaardite and $PdAuCu_2$ grains; Fig. 3*c*) and zvyagintsevite, Pd_3Pb, (as inclusions in two skaergaardite grains; Fig. 3*e*). Several unidentified Cu-Pd-Au-

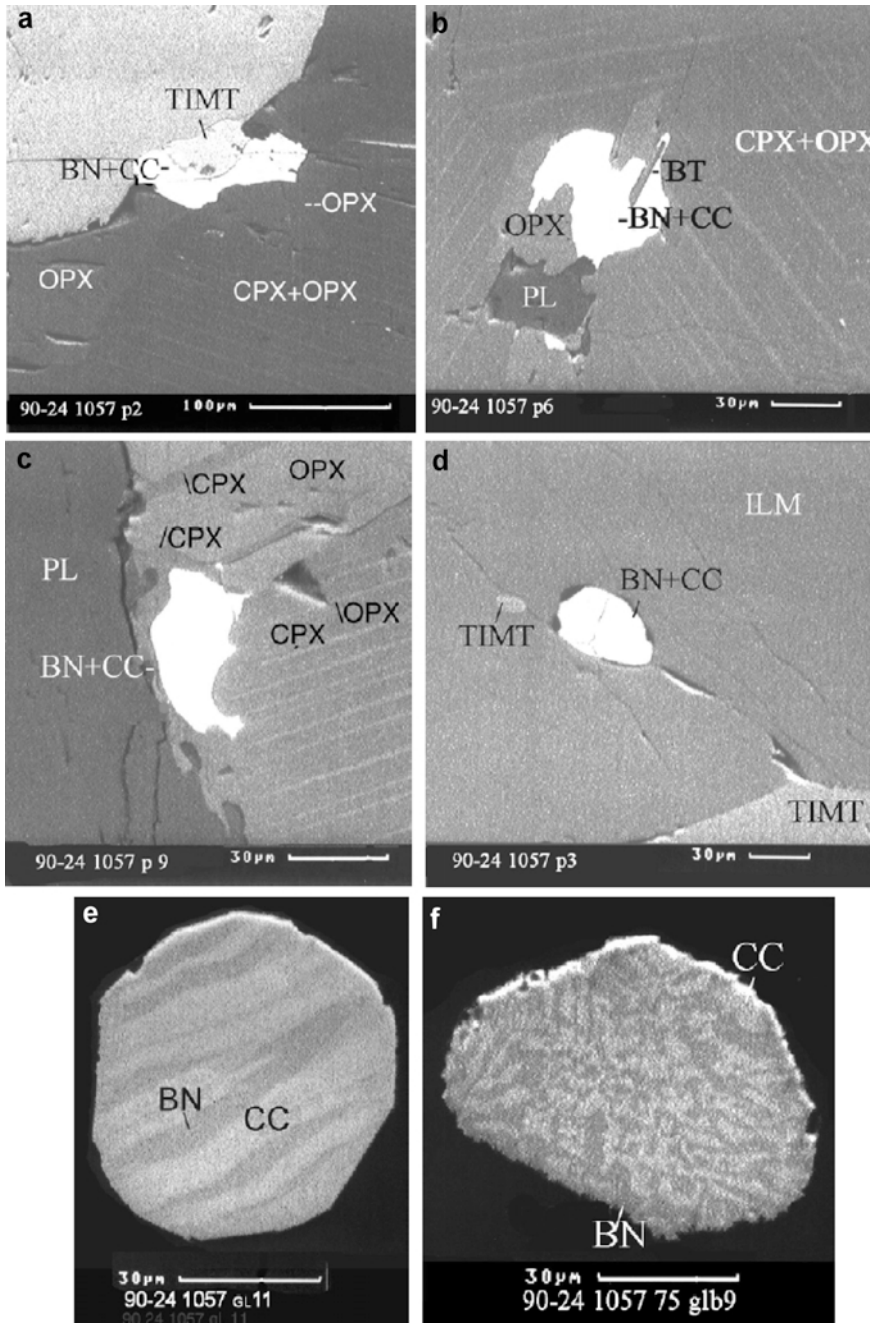

FIG. 1. BSE images of Cu-Fe sulphides, oxides and silicates associated with skaergaardite. (*a*) Typical occurrence of Cu-Fe sulphides (bornite: BN; chalcocite: CC) at interstices between oxides (ilmenite: ILM; titanian magnetite: TITM) and pyroxenes (orthopyroxene: OPX; clinopyroxene: CPX). (*b*) Cu-Fe sulphides intergrown with biotite (BT). (*c*) Irregular Cu-Fe sulphide aggregates (bornite + chalcocite) in pyroxene at the contact with plagioclase (PL). (*d*) A Cu-Fe sulphide microglobule inclusion in ilmenite. (*e*,*f*) Exsolution textures in bornite + chalcocite in liberated microglobules.

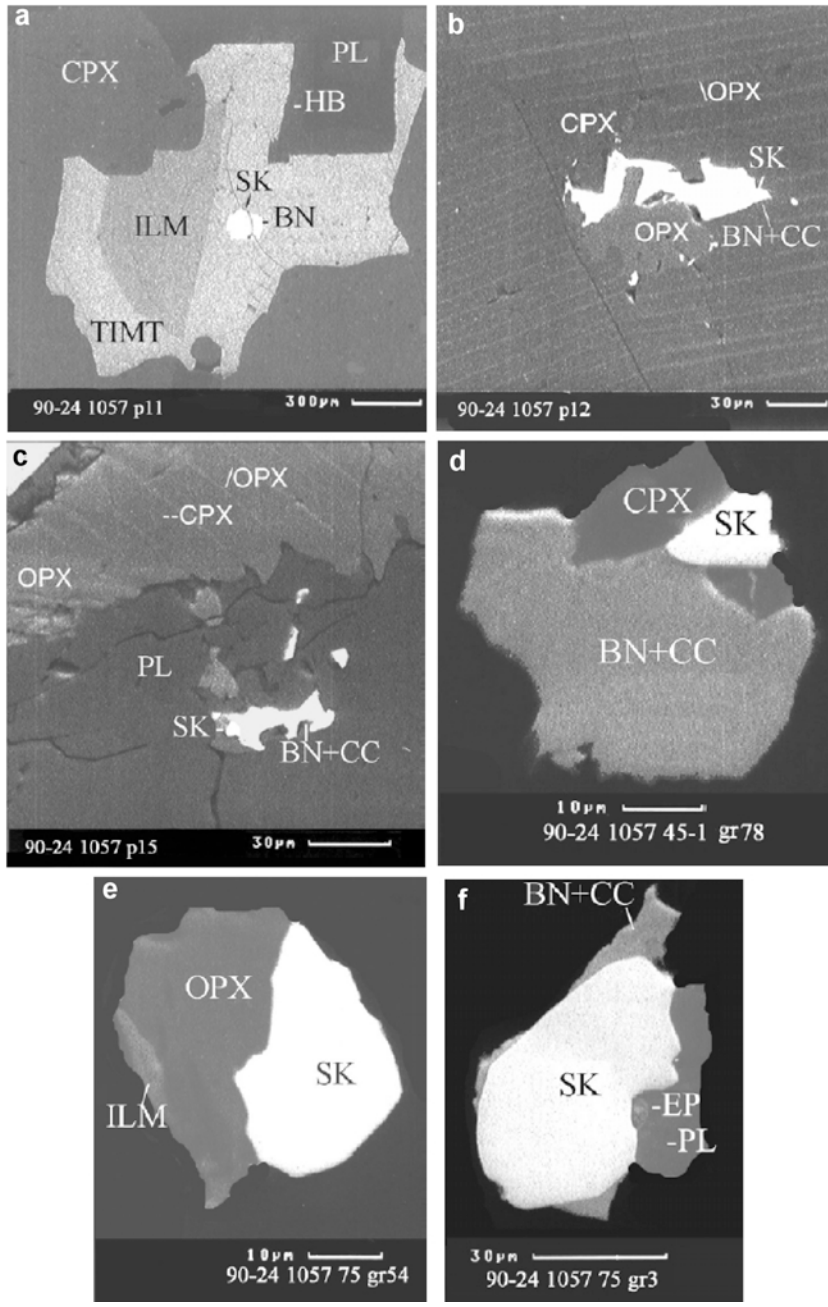

FIG. 2. BSE images of skaergaardite (SK), Cu-Fe sulphides, PGM, and unidentified platinum-group alloys. (*a*) Inclusions of skaergaardite + bornite in titanian magnetite. Associated minerals include ilmenite, clinopyroxene, amphibole (HB) and plagioclase. (*b*) Linear exsolution textures in pyroxenes. Notice the disruption of the exsolution lamellae near Cu-Fe sulphide and skaergaardite (SK) inclusions. (*c*) Skaergaardite and Cu-Fe sulphide (bornite + chalcocite) inclusions in plagioclase. (*d*) Skaergaardite in contact with clinopyroxene (CPX) and bornite-chalcocite intergrowth (BN+CC). (*e*) Subhedral skaergaardite attached to orthopyroxene (OPX) with ilmenite (ILM). (*f*) Sub-rounded skaergaardite associated with plagioclase (PL), epidote (EP) and bornite-chalcocite intergrowth (BN-CC).

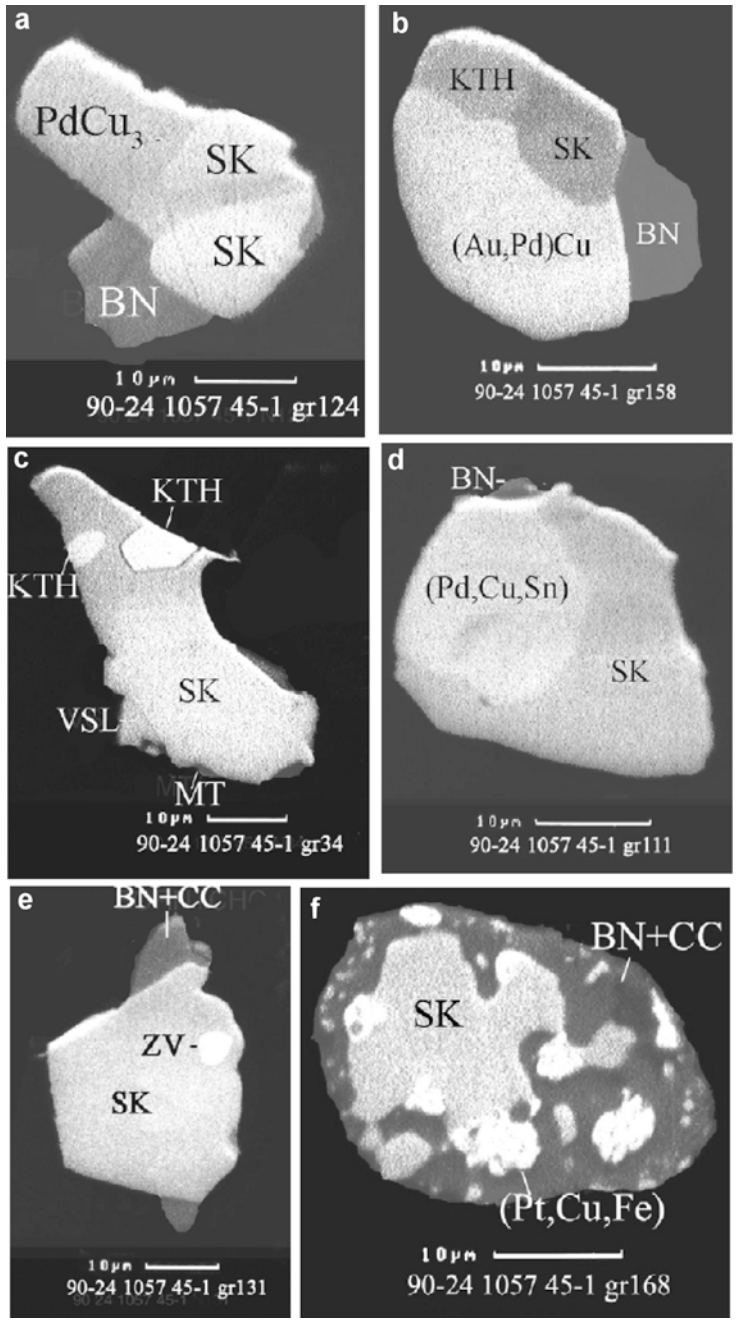

FIG. 3. BSE images of skaergaardite and associated minerals. (*a*) An elongate grain of an unnamed $PdCu_3$ mineral associated with skaergaardite and bornite. (*b*) An unnamed mineral $PdAuCu_2$ [(Au,Pd)Cu] associated with skaergaardite, keithconnite and bornite. (*c*) A liberated grain of skaergaardite associated with keithconnite (KTH) and vasilite (VSL). (*d*) An unidentified (Pd,Cu,Sn) mineral associated with skaergaardite and bornite. (*e*) A subhedral crystal of skaergaardite with a droplet-like inclusion of zvyagintsevite (ZV). (*f*) An irregular aggregate of skaergaardite intergrown with hongshiite? (Pt,Cu,Fe) included in a liberated microglobule of bornite+chalcocite intergrowth.

Pt-Fe alloys have also been observed. They include: (Cu,Pd) and (Cu,Pd,Au) alloys representing ~3% of the total PGM observed; occurring as discrete irregular grains or as intergrowths with skaergaardite grains (Fig. 4*a*), unnamed Au_3Cu, (as an inclusion in a $PdAuCu_2$ grain), unnamed $PdCu_3$ (12 grains + inclusions in seven skaergaardite grains; study in progress; Fig. 3*a*), unnamed $PdAuCu_2$ (Pd-rich tetra-auricupride(?) (five grains + inclusions in four skaergaardite grains; Fig. 3*b*), unnamed (Pd,Cu,Sn) (three grains and inclusions in 12 skaergaardite grains; Fig. 3*d*), along with (Pt,Fe,Cu,Pd)-alloys (tetraferroplatinum? and hongshiite?; Fig. 3*f*), unnamed $(Pt,Pd)Cu_3$ (one inclusion in a skaergaardite grain).

Skaergaardite and other PGM occur in the microglobules as: (1) droplets (Fig. 4*b–f*); (2) cubic grains with rounded outlines (Fig. 5*d*,*f*); (3) euhedral to subhedral grains (Fig. 5*a*,*b*,*c*,*e*); and (4) irregular grains or aggregates (Fig. 4*a*). The contact between PGM and the surrounding Cu-Fe sulphides is generally sharp and distinct. It is also of interest to note that most grains of skaergaardite are inclusion-free (Fig. 4*b–f*; Fig. 5), and in cases where inclusions are noted, they are either $PdCu_3$, (Cu,Pd,Au) alloy, unnamed (Pd,Cu,Sn) or more rarely, keithconnite, (Au,Pd)Cu, vasilite, zvyagintsevite and (Pt,Cu,Fe,Pd) alloys.

Skaergaardite constitutes variable proportions of the sulphide-PGM microglobules. Based on the volume percent occupied, the mineral can be classed into one of three categories of microglobules: (1) those with fine inclusions of the mineral (Fig. 4*b–d*; Fig. 5*a*,*c*); (2) those where skaergaardite comprises ~50% of the volume (Fig. 4*e*; Fig. 5*d–f*); and (3) those dominated (>75% by volume) by the mineral (Fig. 4*a*,*f*). In general, the mineral tends to be localized at the margins of the microglobules (Fig. 4*c*,*d*; Fig. 5*a*,*d*).

Physical and optical properties

Skaergaardite occurs as droplets, equant grains with rounded outlines, subhedral to euhedral crystals and as irregular grains that vary in size from 2 to 75 μm, averaging 22 μm in equivalent circle diameter. When present as subhedral to euhedral grains, crystal faces are evident, some suggesting the presence of the cube {100} (Fig. 5*e*), others more complex forms such as the dodecahedron {110} (Fig. 5*b*). The mineral is steel grey with a bronze tint, has a black streak, a metallic lustre, and is sectile. Neither cleavage nor fracture was observed. The mineral has a microindentation hardness of VHN_{25} = 257 (n = 5 indentations on two grains; range of 244–267 kg/mm^2), which corresponds to a Mohs hardness of 4 to 5. A measured density could not be obtained due to the small size of the grains. Based on the empirical formula and unit-cell parameters refined from X-ray powder diffraction data, the calculated density is 10.64 g/cm^3, a value consistent with many PGM. Under reflected light in air, the mineral is isotropic, non-pleochroic and exhibits neither discernible internal reflections nor evidence of twinning. In association with bornite and chalcopyrite, skaergaardite appears bright creamy white but against the strong blue of digenite and chalcocite, it appears bright white. Reflectance values (Fig. 6) were measured in air and oil (Zeiss oil, n_D = 1.515, DIN 58.884 at 20ºC) relative to a WTiC standard (Zeiss 314) following the methodology of Stanley *et al.* (2002). These data are very close to those of hongshiite (PtCu) to which skaergaardite may be structurally related (Fig. 6). The reflectance data and colour values for the skaergaardite grain that was analysed (75-N58) are given in Table 1.

Chemical composition

Chemical analyses were carried out on more than 300 grains using energy dispersion spectrometry (EDS) and a Camscan Microspec-4DV scanning electron microscope with a Link AN-1000 detector (Tables 2,3). The operating conditions included an accelerating beam voltage of 30 kV, a beam current of 1–2 nA, a beam diameter of 1 μm and counting times of 50–100 s.

In general terms, the mineral is relatively pure in terms of Pd and Cu, although up to seven other elements may be present. The common trace elements that are present in more than 80% of the 311 skaergaardite grains analysed are Fe and Zn, which replace Cu. As a result, the empirical formula for skaergaardite, calculated from the arithmetic average mean in Table 2 (normalized to two a.p.f.u.), is: $(Pd_{0.967}Au_{0.020}Pt_{0.010})_{\Sigma 0.997}(Cu_{0.820}Fe_{0.120}Zn_{0.039}Sn_{0.016}Te_{0.004}Pb_{0.003})_{\Sigma 1.002}$. The simplified formula is PdCu, which requires: Pd 62.61, Cu 37.39, total 100.00 wt.%.

The grain from which the physical and optical data were obtained (75-1, 58) gave the composition in Table 3, analysis 1, and the grain from

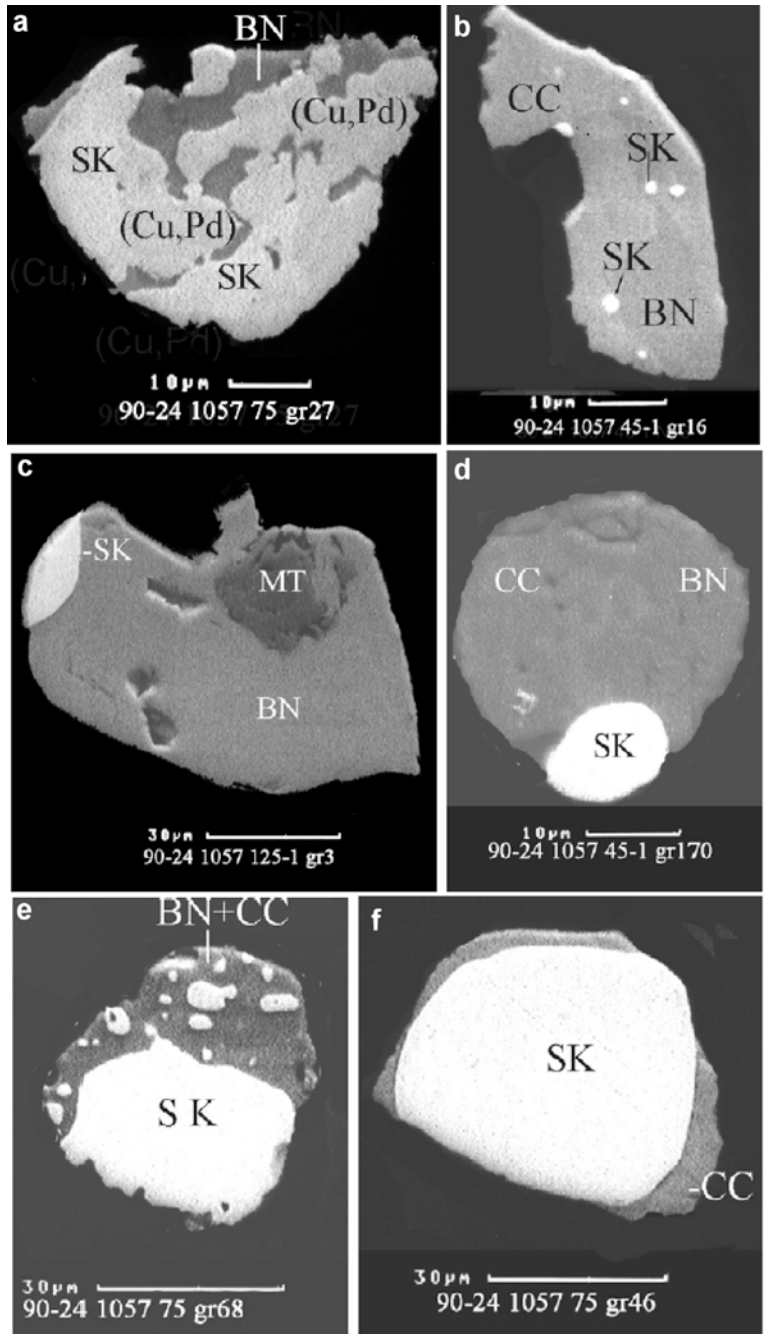

FIG. 4. BSE images of skaergaardite and associated minerals. (*a*) An irregular aggregate of skaergaardite intergrown with $PdCu_3$ (Cu,Pd) and bornite. (*b*) Fine inclusions of skaergaardite in Cu-Fe sulphide microglobules. (*c*) Elongated subhedral grain of skaergaardite attached to bornite with magnetite. (*d*) Liberated microglobule of bornite and chalcocite with rounded skaergaardite typically at the margin. (*e*) A liberated bornite + chalcocite intergrowth microglobule with ~50% (by volume) skaergaardite. (*f*) A liberated chalcocite microglobule with ~90% (by volume) skaergaardite.

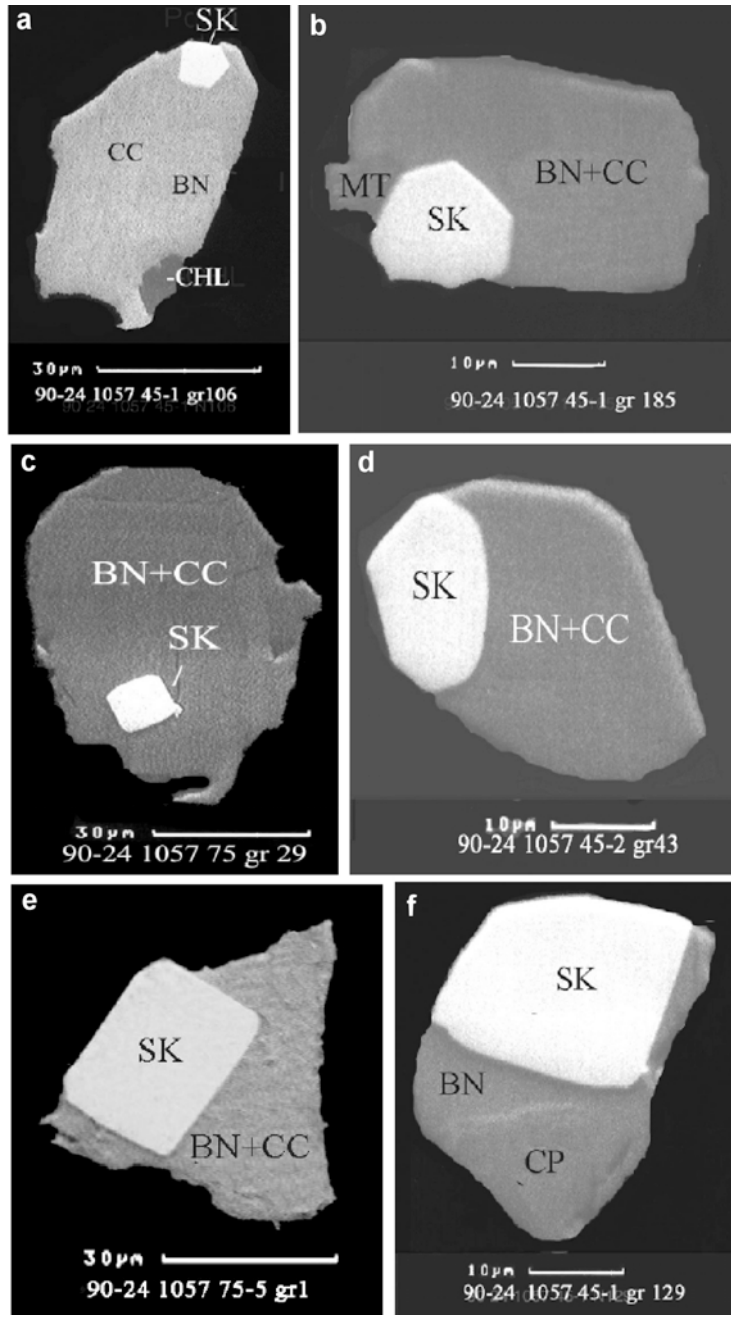

FIG. 5. BSE images of skaergaardite and associated minerals. (*a*) A small skaergaardite inclusion at the edge of a chalcocite + bornite microglobule with attached chlorite. (*b*) A subhedral crystal of skaergaardite exhibiting the dodecahedron {110} or possibly cubo-octahedral forms at the margin of a microglobule of bornite-chalcocite intergrowth and attached magnetite. (*c*) A euhedral crystal of skaergaardite exhibiting the form cube {100}. (*d*) The common occurrence of skaergaardite at the margins of bornite + chalcocite microglobules. (*e*) A euhedral crystal of skaergaardite exhibiting the form cube {100} (possibly distorted) included in a bornite-chalcocite intergrowth. (*f*) A liberated bornite + chalcopyrite microglobule with ~50% (by volume) of a skaergaardite cube with rounded edges.

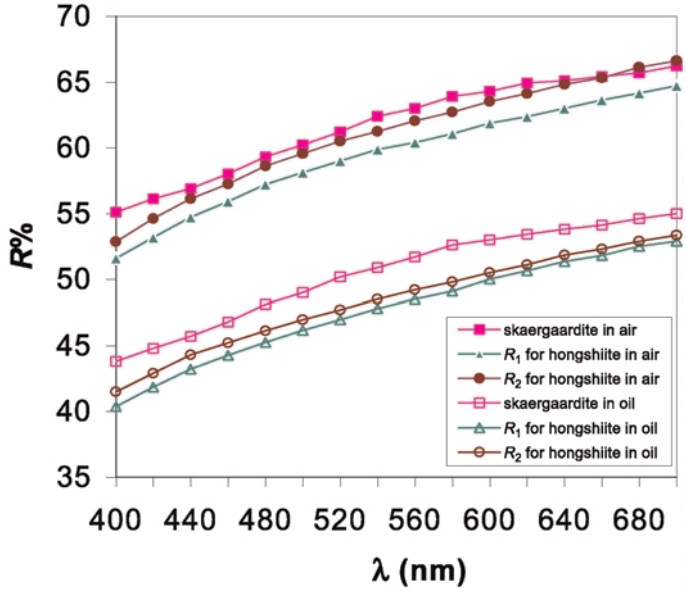

FIG. 6. Reflectance spectra for skaergaardite measure in air (filled squares) and in oil (open squares) compared to data for hongshiite from Brazil (R_1 filled triangles, R_2 filled circles; $^{im}R_1$ open triangles, $^{im}R_2$ open circles; Kwitko *et al.*, 2002).

TABLE 1. Reflectance data (%) and colour values for skaergaardite.

λ	*R*	^{im}R	λ	*R*	^{im}R
400	55.1	43.8	560	63.0	51.7
420	56.1	44.8	580	63.9	52.6
440	56.9	45.7	600	64.3	53.0
460	58.0	46.8	620	64.9	53.4
480	59.3	48.1	640	65.1	53.8
500	60.2	49.0	660	65.4	54.1
520	61.2	50.2	680	65.7	54.6
540	62.4	50.9	700	66.2	55.0
COM minimum wavelengths					
470	58.65	47.4	589	64.1	52.8
546	62.6	51.1	650	65.25	53.95
Colour values: A Illuminant (~2856 K)					
x	0.32	0.322	λ_d	577	577
y	0.326	0.328	P_e%	5.3	6.3
Y%	62.7	51.4			
Colour values: C Illuminant (~6774 K)					
x	0.456	0.457	λ_d	586	586
y	0.411	0.411	P_e%	7.7	7.7
Y%	63.3	52.0			

TABLE 2. Chemical composition of skaergaardite from Greenland.

Element	Wt.%	Range	Stand. dev.	Standards used	X-ray line used
Pd	58.94	33.0–64.4	5.39	Pd	Pd-*L*α
Pt	1.12	n.d.–12.7	2.01	Pt	Pt-*L*α
Au	2.23	n.d.–31.5	5.26	Au	Au-*L*α
Cu	29.84	15.8–43.5	2.46	Cu	Cu-*K*α
Fe	3.85	n.d.–7.3	1.87	Fe	Fe-*K*α
Zn	1.46	n.d.–7.2	1.02	Zn	Zn-*K*α
Sn	1.08	n.d.–21.4	2.72	Sn	Sn-*L*α
Te	0.28	n.d.–4.7	0.70	PbTe	Te-*L*α
Pb	0.39	n.d.–5.5	0.82	PbTe	Pb-*M*α
Total	99.19				

which the X-ray powder diffraction data were obtained (125-1, 4) gave the composition in Table 3, analysis 2.

Factor-loading plot diagrams for the general selection of skaergaardite analyses (311 analyses) shows four statistically contrasting compositional groups (Figs 7 and 8): (1) characteristic elements – Pd, Fe and Zn (Factor 1) – e.g. Table 3, analysis 1–8; (2) characteristic elements – Cu, Au and Te (Factor 1) – e.g. Table 3, analysis 9–16; (3) characteristic elements – Sn and Pb (Factor 2) – e.g. Table 3, analysis 18–30; (4) characteristic elements – Pt, less common Sn and Fe (Factor 3) – e.g. Table 3, analysis 17–24.

The first group of analyses includes >80% of skaergaardite compositions – these are Pd compositions where the Au and Pt contents are very small. The variation of chemical compositions of these skaergaardites is based on the replacement Cu ⇌ (Fe,Zn) only.

The second group consists of Au- and Te-rich skaergaardite grains. The characteristic isomorphic replacements in these compositions of skaergaardites are Pd ⇌ Au (up to 31.5 wt.% Au) and Cu ⇌ Te (up to 4.7 wt.% Te), simultaneously. This group, as a rule, is poor in Fe and Zn.

The third group is characterized by skaergaardite compositions that are rich in Sn and Pb. The

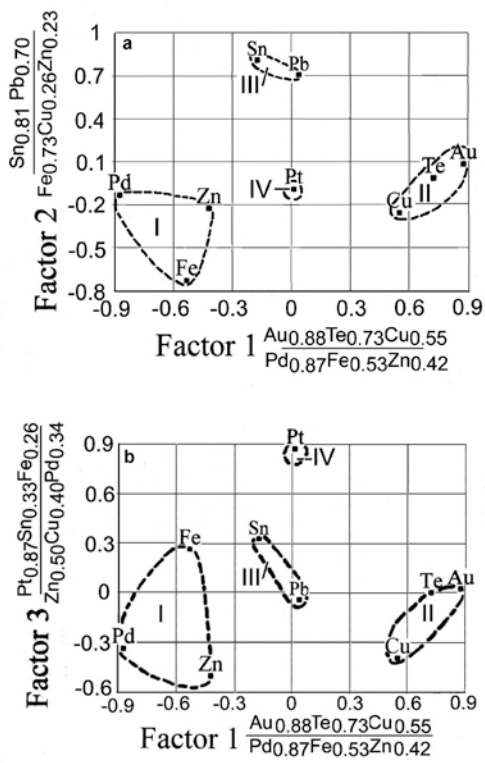

FIG. 7. Factor analysis diagrams for two combinations of elements showing the four groups.

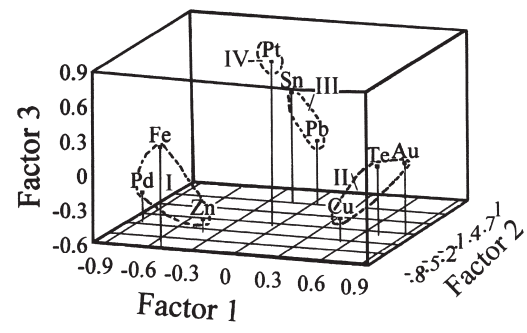

FIG. 8. Factor analysis diagrams showing the four groups in three-dimensional space.

TABLE 3. Selected electron probe microanalyses of skaergaardite.

Element	Analyses of different skaergaardite grains							
	1	2	3	4	5	6	7	8
	75-1,58	125-1,4	P.s.,5	45-1,5	45-1,22	45-1,24	45-1,77	45-1,171
Pd	62.3	62.2	62.1	63.6	61.9	62.3	62.6	62.7
Pt	n.d.	n.d.	n.d.	n.d.	n.d.	n.d.	n.d.	n.d.
Au	n.d.	1.2	n.d.	n.d.	n.d.	n.d.	n.d.	n.d.
Cu	30.2	28.0	29.5	29.3	30.4	30.2	30.3	29.5
Fe	3.9	4.6	5.4	5.0	6.6	5.8	6.2	5.8
Zn	1.5	1.9	1.6	2.6	n.d.	1.4	n.d.	1.3
Sn	0.9	1.1	n.d.	n.d.	n.d.	n.d.	n.d.	3.14
Te	n.d.	n.d.	n.d.	n.d.	n.d.	n.d.	n.d.	n.d.
Pb	n.d.	n.d.	n.d.	n.d.	n.d.	n.d.	n.d.	n.d.
Total	98.8	99.4	98.6	100.5	98.9	99.7	99.1	99.3
Pd	1.008	1.018	0.998	1.006	0.987	0.987	1.000	1.001
Pt	0.000	0.000	0.000	0.000	0.000	0.000	0.000	0.000
Au	0.000	0.011	0.000	0.000	0.000	0.000	0.000	0.000
ΣAtoms	1.008	1.029	0.998	1.006	0.987	0.987	1.000	1.001
Cu	0.819	0.763	0.794	0.776	0.812	0.801	0.811	0.789
Fe	0.120	0.143	0.165	0.151	0.201	0.175	0.189	0.176
Zn	0.040	0.050	0.042	0.067	0.000	0.036	0.000	0.034
Sn	0.013	0.016	0.000	0.000	0.000	0.000	0.000	0.000
Te	0.000	0.000	0.000	0.000	0.000	0.000	0.000	0.000
Pb	0.000	0.000	0.000	0.000	0.000	0.000	0.000	0.000
ΣAtoms	0.992	0.972	1.001	0.994	1.013	1.012	1.000	0.999

Element	Analyses of different skaergaardite grains							
	9	10	11	12	13	14	15	16
	P.s.,1	45-1,16	45-1,25	45-1,91*	45-1,91*	45-1,158	45-1,179*	45-1,179*
Pd	58.1	56.1	58.3	51.8	35.3	44.0	33.0	51.5
Pt	1.1	n.d.	1.2	n.d.	n.d.	3.0	1.2	1.2
Au	4.7	8.4	2.2	10.9	30.7	18.6	31.5	10.9
Cu	28.1	30.6	29.6	31.6	29.9	31.1	28.4	30.4
Fe	6.0	2.4	2.2	0.6	n.d.	1.4	1.3	2.2
Zn	1.5	2.0	1.1	n.d.	n.d.	1.1	0.5	1.3
Sn	n.d.	1.1	3.2	1.0	n.d.	n.d.	n.d.	3.14
Te	n.d.	n.d.	n.d.	1.2	2.4	n.d.	2.3	0.9
Pb	n.d.	n.d.	1.9	1.8	n.d.	n.d.	1.1	1.1
Total	99.5	99.5	99.7	98.9	98.3	99.2	99.3	99.5
Pd	0.951	0.937	0.975	0.904	0.679	0.784	0.635	0.884
Pt	0.010	0.000	0.011	0.000	0.000	0.029	0.012	0.011
Au	0.042	0.076	0.020	0.103	0.319	1.179	0.327	0.101
ΣAtoms	1.003	1.013	1.006	1.007	0.998	0.992	0.974	0.996
Cu	0.770	0.856	0.829	0.924	0.963	0.928	0.915	0.873
Fe	0.187	0.076	0.070	0.020	0.000	0.048	0.048	0.072
Zn	0.040	0.054	0.030	0.000	0.000	0.032	0.016	0.036
Sn	0.000	0.000	0.048	0.016	0.000	0.000	0.000	0.000
Te	0.000	0.000	0.000	0.017	0.039	0.000	0.037	0.013
Pb	0.000	0.000	0.016	0.016	0.000	0.000	0.011	0.010
ΣAtoms	0.997	0.986	0.993	0.993	1.002	1.008	1.027	1.004

TABLE 3 (*contd.*)

Element	Analyses of different skaergaardite grains							
	17	18	19	20	21	22	23	24
	45-1,3	45-1,21	45-1,23	45-1,71	45-1,78	45-1,138	45-1,156	125-1,9
Pd	57.1	54.2	55.5	58,5	53.4	56.8	53.7	54.7
Pt	4.3	3.8	8.7	4.9	10.0	6.6	10.1	10.0
Au	n.d.	3.7	n.d.	n.d.	n.d.	1.0	n.d.	n.d.
Cu	29.7	29.3	28.1	29.2	28.8	30.6	26.7	27.9
Fe	2.2	1.4	5.4	6.2	6.9	5.5	4.5	6.3
Zn	1.8	0.8	1.9	0.8	0.6	1.0	1.2	0.7
Sn	n.d.	2.3	3.2	n.d.	n.d.	n.d.	1.1	n.d.
Te	n.d.	n.d.	n.d.	n.d.	n.d.	n.d.	n.d.	n.d.
Pb	3.2	3.5	1.9	n.d.	n.d.	n.d.	1.7	n.d.
Total	98.3	99.0	99.6	99.6	99.7	101.5	99.0	99.6
Pd	0.968	0.941	0.920	0.950	0.881	0.914	0.923	0.912
Pt	0.040	0.036	0.079	0.043	0.090	0.058	0.095	0.091
Au	0.000	0.035	0.000	0.000	0.000	0.009	0.000	0.000
ΣAtoms	1.008	1.012	0.999	0.993	0.971	0.981	1.018	1.003
Cu	0.843	0.852	0.780	0.794	0.796	0.825	0.769	0.779
Fe	0.071	0.046	0.170	0.192	0.217	0.169	0.147	0.200
Zn	0.050	0.023	0.051	0.021	0.016	0.026	0.034	0.019
Sn	0.000	0.036	0.000	0.000	0.000	0.000	0.017	0.000
Te	0.000	0.000	0.000	0.000	0.000	0.000	0.000	0.000
Pb	0.028	0.031	0.000	0.000	0.000	0.000	0.015	0.000
ΣAtoms	0.998	0.987	1.001	1.007	1.029	1.020	0.982	0.998

Element	Analyses of different skaergaardite grains					
	25	26	27	28	29	30
	45-1,18	45-1,168	45-1,87	45-1,118	45-1,144	45-1,137
Pd	58.7	55.7	56.7	58,3	56.2	44.7
Pt	1.6	4.2	n.d.	1.0	2.7	12.7
Au	1.3	n.d.	n.d.	n.d.	n.d.	n.d.
Cu	30.3	30.1	18.8	30.3	27.9	19.3
Fe	1.6	0.9	2.0	1.1	0.8	1.5
Zn	0.7	0.4	n.d.	n.d.	n.d.	n.d.
Sn	5.2	6.2	20.5	7.6	9.6	21.4
Te	n.d.	n.d.	n.d.	n.d.	n.d.	n.d.
Pb	n.d.	1.3	1.1	1.0	2.2	n.d.
Total	99.4	98.8	99.1	99.3	99.4	99.3
Pd	0.979	0.952	1.022	0.980	0.972	0.844
Pt	0.015	0.039	0.000	0.009	0.025	0.131
Au	0.012	0.000	0.000	0.000	0.000	0.000
ΣAtoms	1.006	0.991	1.022	0.989	0.997	0.975
Cu	0.847	0.862	0.568	0.853	0.808	0.610
Fe	0.051	0.029	0.069	0.035	0.026	0.054
Zn	0.019	0.011	0.000	0.000	0.000	0.000
Sn	0.078	0.095	0.331	0.114	0.149	0.362
Te	0.000	0.000	0.000	0.000	0.000	0.000
Pb	0.000	0.011	0.010	0.009	0.020	0.000
ΣAtoms	0.995	1.008	0.978	1.011	1.003	1.026

Analyses 1−8 represent the dominant compositional group; analyses 9−16 represent Au-rich compositions of skaergaardite (*two zones in one grain of skaergaardite); analyses 17−24 represent Pt-rich compositions of skaergaardite; analyses 25−30 represent Sn-rich compositions of skaergaardite.

scheme of isomorphic replacement (Cu,Fe,Zn) ⇌ (Sn,Pb) (Sn up to 21.4 wt.%, Pb up to 5.5 wt.%) is noted for the compositions of this group of skaergaardite. As a result, these skaergaardites are usually poor in Cu, Fe and Zn.

The fourth group includes Pt-rich compositions of skaergaardite (up to 12.7 wt.% Pt), as well as those that are rich in Fe and Sn. The isomorphic replacements here are described by the following replacement schemes: Pd ⇌ Pt and Cu ⇌ (Fe,Sn), simultaneously.

The defined compositional groups of skaergaardite and associated PGM and Au minerals are correlated as follows: (1) skaergaardite enriched by Au-(Te) coexists with Au minerals and keithconnite (Fig. 3*b*); (2) skaergaardite enriched with Sn-(Pb) coexists with (Pd,Cu,Sn) alloy and zvyagintsevite (Fig. 3*d*,*e*); and (3) skaergaardite enriched with Pt coexists with Pt-Fe-Cu-Pd alloys (Fig. 3*f*).

X-ray crystallography

X-ray powder-diffraction data (Table 4) were collected with a 114.6 diameter Gandolfi camera employing Ni-filtered Cu-*K*α radiation (λ = 1.5418 Å). Skaergaardite is considered to be isostructural with synthetic CuZn (space-group *Pm*3*m*) based on similarities in their X-ray powder patterns and compositions (i.e. both are *AX* compounds). Synthetic CuZn (β-brass) is considered to be ordered with the CsCl crystal-structure (Nowotny and Winkels, 1939). On this basis, skaergaardite crystallizes in the space-group *Pm*3*m* with V = 27.0378 Å^3 and Z = 1. The Pearson Symbol Code (*PSC*) is *cP*2. The unit-cell edge, a = 3.0014(2) Å, was determined on the basis of 11 reflections for which unambiguous indexing was possible. The observed intensities were determined from a scanned PXRD film. These are in good agreement with those calculated using the program *Powdercell* (Nolze and Kraus, 1998), the refined unit-cell edge, and assuming skaergaardite to have the CsCl structure [Pd in 1*a*, ($Cu_{0.8}Fe_{0.2}$) in 1*b*]. Evidence to support metal ordering can be found in the calculated powder diffraction pattern: several weak reflections (e.g. 100, 111, 210, etc.) have I_{calc} = 0 when a complete disordering scenario is considered.

Table 4. Skaergaardite and related minerals: X-ray powder diffraction data.

Skaergaardite					Synthetic CuZn[1]			Hongshiite[2]		
I_{meas}	I_{calc}	d_{meas} (Å)	d_{calc} (Å)	*hkl*	*I*	d_{meas} (Å)	*hkl*	*I*	d_{meas} (Å)	*hkl*
								30	4.35	021
5	8	3.003	3.001	100	6	2.95	100	20	3.03	300
								10	2.295	205
100	100	2.122	2.122	110	100	2.08	110	100	2.199	006
								80	1.895	404
5	2	1.732	1.733	111	1	1.702	111	<10	1.738	241
20	15	1.5000	1.5006	200	15	1.474	200	10	1.489	416
5	3	1.3427	1.3423	210	2	1.319	210	50	1.350	048
								50	1.325	309
50	30	1.2254	1.2253	211	29	1.203	211	<10	1.290	072
								80	1.148	4010
5	10	1.0607	1.0612	220	5	1.042	220	30	1.099	00$\overline{12}$
1	1	1.0009	1.0005	221	1	0.983	300	20	0.986	8$\overline{23}$
20	18	0.9491	0.9491	310	8	0.932	310	10	0.948	808
					1	0.889	311	30	0.879	0015
10	7	0.8666	0.8664	222	5	0.851	222	30	0.868	11$\overline{15}$
								50	0.856	9$\overline{30}$
								30	0.842	755
70	65	0.8021	0.8022	321	3	0.788	321			
					4	0.738	400			

[1] Nowotny and Winkels (1939). [2] Yu (2001)

Related structures

As has been noted, skaergaardite is isostructural with synthetic CuZn, which crystallizes in the space group *Pm*3*m* (Nowotny and Winkels, 1939). Synthetic CuZn has been loosely considered as being equivalent to zhanghengite (e.g. Bayliss *et al*., 2001), a mineral known only from the Boxian meteorite (Wang, 1986). This comparison is inaccurate however, as Cu and Zn are disordered in zhanghengite, resulting in the mineral crystallizing in the space group *Im*3*m*. Skaergaardite may also be isostructural with wairauite, CoFe (Challis and Long, 1964), but this can only be considered as a working hypothesis, as no X-ray diffraction data exist for wairauite, and only partial data (i.e. no corresponding intensity data) are available for synthetic CoFe (Ellis and Greiner, 1941). Skaergaardite may also be structurally related to hongshiite (PtCu), which is reported to be hexagonal (diffraction symmetry *R***; Yu, 2001). It should be noted that while the name hongshiite is in common usage for alloys of PtCu composition, the mineral has not been formally accepted by the IMA-CNMMN (Cabri, 2002, p. 48; Jambor and Grew, 1990). To further complicate matters, a mineral has been described from the Itabira district, Brazil, which appears to correspond to hongshiite (Kwitko *et al*., 2002). The mineral gives an X-ray diffraction pattern consistent with hongshiite (Yu, 2001), but has two additional, unindexable diffraction lines (Kwitko *et al*., 2002). Further studies are clearly required to fully characterize hongshiite and to elucidate its true relationship with skaergaardite.

Other possible occurrences of skaergaardite

Komppa (1998) reported 90 grains of an unknown PdCu alloy in a drill core (DU-15) from the South Kawishiwi Intrusion of the Duluth Layered Intrusion Complex, Minnesota, USA (Saini-Eidukat *et al*., 1990). The mineral may be equivalent to skaergaardite, but no XRD studies were performed on the material. The Duluth intrusion is composed of several separate intrusions, which discharged *via* the Mid-continent Rift System ~1100±15 Ma ago, and is characterized by the occurrence of different mineralization containing Cr-Fe-Ti-V oxides, Cu-Ni sulphides and PGE in the troctolitic South Kawishiwi Intrusion on its western and northern edges. Of the PGM, the chemistry of which was determined quantitatively, 26% were a PdCu alloy, 26% were Pt-Fe alloys and 34% consisted of various other Pd minerals. Half the PdCu alloys occur associated with base metal sulphides (pentlandite, chalcopyrite, bornite or chalcocite), 24% with silicates, 10% with oxides, and 16% at silicate-oxide margins. The PdCu alloys form composite grains with Pt-Fe alloys or Pd tellurides, arsenides, Ag sulphides and Pb alloys, with individual grains relatively large with respect to other PGM, having a mean area of >100 μm^2, and ranging from 0.3 to 442 μm^2. The mineral is reported to contain varying amounts of Pt, Au, Ag or Ru substituting for Pd and Cu is usually replaced by Fe, and to a lesser extent by Ni, As, Te, Sn or Pb. Selected analyses from U. Komppa's thesis are given in Table 5, with concentrations given in wt.%, based on 2 a.p.f.u. More details of Komppa's work can be found in a translation of her thesis at: http://www.nrri.umn.edu/egg/download/Thesis_PGMs_in_the_Duluth_Complex.zip.

Andersen *et al*. (1998) reported that an alloy "stoichiometrically close to (Cu,Fe)(Au,Pd,Pt)" is the predominant precious metal mineral in the Platinova Reefs, Skaergaard intrusion. Six of nine electron probe microanalyses given in their Table 3 are compositionally similar to our analyses and could be skaergaardite. Andersen *et al*. (1998) also show photomicrographs of sulphide microglobules with Pd-rich alloys at their margins that have crystal faces within the sulphides, such as shown in Fig. 5*b*. They interpret this texture as indicating that the alloy "nucleated on the silicate surface and grew into a liquid sulphide droplet."

Power *et al*. (2000) report that Pd-Cu alloys are among one of nine dominant PGM from the layered intrusion on Rum, Scotland. They include a semi-quantitative analysis, which may be calculated to be $Pd_{0.94}(Cu_{0.76}Fe_{0.17}Zn_{0.12}Ni_{0.01})_{\Sigma 1.06}$ on the basis of 2 a.p.f.u.

Genetic implications and discussion

The Pd-Cu binary for Cu atomic concentrations of $0.43 < x < 0.70$ over the range $525 < T < 1800$ K has been determined (Fig. 9; Baker *et al*., 1992). For this compositional range, the solidus develops between 1400 and 1500 K, depending on the Pd:Cu ratio (increasing proportional to the Pd atomic concentration). Below the solidus, PdCu with a face-centred cubic (*fcc*) structure develops. The structure is disordered, although limited long-

TABLE 5. Selected electron probe microanalyses of PdCu (Komppa, 1998).

	1	2	3	4	5	6	7	8
Pd	61.15	60.6	62.06	63.08	59.55	50.35	54.60	57.92
Pt	n.d.	2.03	n.d.	n.d.	4.61	4.92	7.56	6.52
Au	n.d.	n.d.	n.d.	n.d.	n.d.	10.02	2.85	n.d.
Cu	33.90	29.50	28.51	29.25	31.79	29.43	28.02	29.04
Fe	4.79	5.85	8.03	7.10	3.69	2.42	3.73	3.60
Ni	n.d.	n.d.	1.77	n.d.	n.d.	n.d.	n.d.	n.d.
As	n.d.	n.d.	n.d.	n.d.	n.d.	1.37	1.96	3.14
Sn	n.d.	n.d.	n.d.	n.d.	n.d.	1.01	2.02	n.d.
Total	99.84	97.98	100.37	99.43	99.64	99.52	100.74	100.22
Pd	0.96	0.99	0.97	1.00	0.97	0.87	0.92	0.95
Pt	0.00	0.02	0.00	0.00	0.04	0.05	0.07	0.06
Au	0.00	0.00	0.00	0.00	0.00	0.09	0.03	0.00
ΣAtoms	0.96	1.01	0.97	1.00	1.01	1.01	1.02	1.01
Cu	0.89	0.81	0.74	0.78	0.87	0.86	0.79	0.80
Fe	0.14	0.18	0.24	0.22	0.11	0.08	0.12	0.11
Ni	0.00	0.00	0.05	0.00	0.00	0.00	0.00	0.00
As	0.00	0.00	0.00	0.00	0.00	0.03	0.05	0.07
Sn	0.00	0.00	0.00	0.00	0.00	0.02	0.03	0.00
ΣAtoms	1.03	0.99	1.03	1.00	0.98	0.99	0.99	0.98

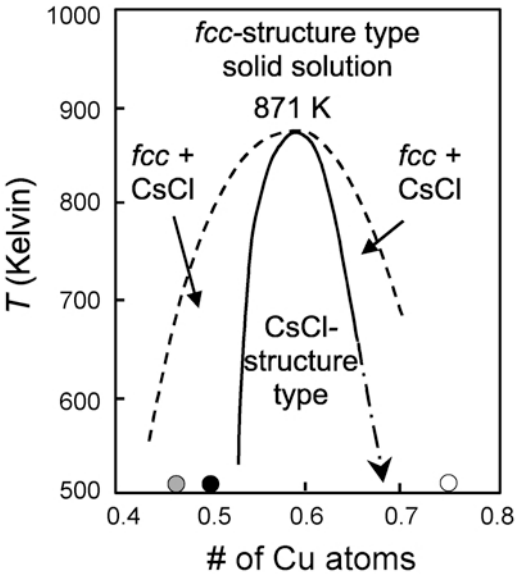

FIG. 9. The phase diagram for Pd-Cu (after Baker *et al*., 1992). The dash-dot arrow indicates a hypothetical extrapolation. The grey circle represents the average Pd:Cu ratio for skaergaardite, the black circle, a ratio of 0.5 and the open circle, a ratio of 0.25 (the latter corresponding to the composition Cu_3Pd).

range ordering may occur (Bruno *et al*., 2001). The *fcc* structure can also be considered geometrically as a tetragonal body-centred (*bcc*) structure (Fig. 10*a*). As *T* decreases, ordering of Cu and Pd atoms is favoured, with a completely ordered structure of the CsCl-structure type developing below 871 K. PdCu having the CsCl structure is also referred to as B2 or β-PdCu, and may be considered (geometrically) as possessing a *bcc*-type lattice (Fig. 10*b*). For compositions corresponding to $0.53 < x < 0.65$ (possibly to $x < 0.68$), only the CsCl-structure type is present, whereas a combination of the CsCl- and disordered *fcc*-structure types exist for compositions between $0.43 < x < 0.53$ and $0.65 < x < 0.70$ (possibly to $x < 0.75$) (Fig. 9). It is interesting to note that the average Pd:Cu ratio observed in skaergaardite (~0.54) plots very close to the solvus separating only the CsCl-structure type *vs.* both the CsCl- and disordered *fcc*-structure types being present (Fig. 10). While it would be enticing to suggest that data from the Pd-Cu binary is sufficient to hypothesize on the conditions under which skaergaardite developed, it is also clear that the concentration of Fe in the mineral is far from insignificant in skaergaardite from both Greenland and Minnesota. For

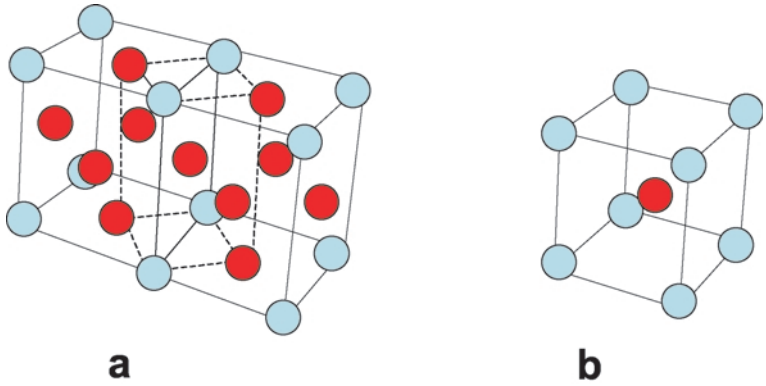

FIG. 10. (*a*) The *fcc*-structure type. A body-centered (*bcc*) tetragonal lattice is noted in dashed lines. (*b*) The CsCl-structure type.

example, the average Cu:Fe ratio in material from Greenland is ~8:2 and ranges from 8:2 to 9:1 for the Duluth mineral. Given the difference in electronic configurations of Cu and Fe, it is therefore probably more appropriate to consider the mineral within the context of the Pd-Cu-Fe ternary system. Unfortunately, no information appears to be available for this particular ternary system. Finally, it is interesting to note that when alloys of composition CoFe (i.e. wairauite) are slowly cooled below a critical T of 700ºC, the CsCl-type structure (i.e. *bcc*) is produced (Ellis and Greiner 1941).

A phase with the composition Pd(Cu,Fe) has been synthesized by Kravchenko and Kolonin (1996), who investigated the Cu-Fe-S system between 45 and 50 at.% S at T = 600ºC, specifically targeting the stability region of intermediate solid solution (ISS). Using annealed samples, the authors found that between $\log f_{S_2}$ values 13 and 7, Pd(Cu,Fe) was produced in association with bornite, and either pyrrhotite or native Cu ($\log f_{S_2}$ = 10−13), pyrrhotite and ISS ($\log f_{S_2}$ = 8−9) or just ISS ($\log f_{S_2}$ = 7−8). No information on the structure of phase(s) produced by these experiments is available. Furthermore, below $\log f_{S_2}$ = 7, a combination of Pd_3Fe, Pd-bearing bornite or PdS were produced. These experimental data are interesting in that they suggest that skaergaardite may develop under conditions of relatively high f_{S_2}. At the same time, minerals believed to be structurally related to skaergaardite (e.g. wairauite and zhanghengite) have clearly developed under conditions of extremely low f_{S_2} (zhanghengite in a meteorite associated with taenite, kamacite, wüstite, troilite, etc.; Wang, 1986; wairauite during serpentinization of an ultramafic intrusion; Challis and Long, 1964).

Skaergaardite in the Skaergaard intrusion, along with the associated PGM and various Cu-Fe sulphides, occurs interstitial to, or as inclusions in rims of primocryst phases (Bird *et al*., 1991) or in rock-forming minerals (pyroxenes, plagioclase, Fe-Ti-oxides), crystallized from intercumulus melt. This suggests that the PGM and sulphides formed during crystallization of intercumulus melt. The rounded to droplet-like morphology of the Cu-Fe sulphide microglobules is strong evidence that they are immiscibility products. As many of the PGM inclusions have similar rounded grain boundaries within the Cu-Fe sulphides, two immiscible melts may have been present: (1) a distinct Cu-Fe sulphide melt; and (2) an alloy melt, enriched in Pd and Cu that separated from the Cu-Fe sulphide melt. Alternatively, the alloy melt is the product of fractionation of Cu-sulphides and liquidus PdCu alloy from the immiscible PGE-bearing and Cu-rich sulphide melt (Karup-Møller and Makovicky, 1999). Most of the Fe-Ti oxides have crystallized after the principal rock-forming minerals (plagioclase and clinopyroxene), being products of a residual melt that accumulated between the latter minerals. This metal-rich residual phase was probably hydrated, given that the Fe-Ti oxides, PGM and Cu-Fe sulphides are, in general, spatially related to H_2O-bearing silicates (e.g. chlorite, micas, amphiboles, epidote-group minerals, etc.). That some PGM occur as inclusions in these oxides and that there exists a spatial relationship between PGM and Fe-Ti oxides further suggests that some metals (notably PGE and Au) and S were fractionated

along with some of the Fe-Ti-oxide cumulus phases during magmatic crystallization. It is relevant to note that Makovicky (2002, p. 140) states "Karup-Møller and Makovicky (1999) stress that the alloy crystallizing from the sulphide liquid together with digenite will have the composition $Cu_{59.4}Pd_{40.6}$ at 900ºC, shifting to $Cu_{55.9}Pd_{44.0}$ at 725ºC. Below solidus, this association is replaced by the assemblage digenite, $Pd_{2.2}S$-alloy; this alloy being $Cu_{51.5-52.6}Pd_{45.6-45.9}S_{2.6-1.8}$ at 550ºC and 400ºC." Hence, the tendency is for compositions of alloy to come closer to the ideal PdCu stoichiometry of 1:1. Data from the Pd-Cu binary indicate that skaergaardite may be the product of solid-state ordering, initially having a disordered (Pd,Cu) *fcc*-structure type at high (possibly magmatic) *T*, and subsequently adopting an ordered CsCl-structure type below 871 K (~600ºC). This conclusion is confirmed by finding rare grains of (Cu,Pd) and (Cu,Pd,Au) non-stoichiometric alloys in the studied sample that are, sometimes, intergrown with skaergaardite (Fig. 4*a*).

Acknowledgements

We are grateful to A.M. Clark for his review and constructive comments. Financial support, provided through a grant to AMM from the Natural Sciences and Engineering Research Council, is gratefully acknowledged. We also acknowledge helpful comments made by members of the CNMMN. Troels D.F. Nielsen publishes with the permission of the Geological Survey of Demark and Greenland, Copenhagen, Denmark. LJC acknowledges technical support provided by CANMET/MMSL, during his tenure as Emeritus Research Scientist.

References

Andersen, J.C.Ø, Rasmussen, H., Nielsen, T.F.D. and Rønsbo, J.G. (1998) The Triple Group and the Platinova gold and palladium reefs in the Skaergaard intrusion: stratigraphic and petrographic relations. *Economic Geology*, **93**, 488–509.

Baker, H., Okamoto, H., Henry, S.D., Davidson, G.M., Fleming, M.A., Kacprzak, L. and Lampman, H.F. (1992) *Alloy Phase Diagrams*. American Society for Metals, Metals Park, Ohio, USA.

Bayliss, P., Bernstein, L.R., McDonald, A.M., Roberts, A.C., Sabina, A.P. and Smith, D.K. (2001) *Mineral Powder Diffraction File Data Book, Sets 1–50*. International Centre for Diffraction Data.

Bird, D.K., Brooks, C.K., Gannicott, R.A. and Turner, P.A. (1991) A gold-bearing horizon in the Skaergaard Intrusion, East Greenland: *Economic Geology*, **86**, 1083–1092.

Bruno, E., Ginatempo, B. and Giuliano, E.S. (2001) Fermi surface incommensurate nestings and phase equilibria in Cu-Pd alloys. *Physical Review B*, **63**, 174107-1–8.

Cabri, L.J. (2002) The platinum-group minerals. Pp. 13–129 in: *The Geology, Geochemistry, Mineralogy and Mineral Beneficiation of the Platinum-Group Elements* (L.J. Cabri, editor). Special Volume **54**, Canadian Institute of Mining, Metallurgy and Petroleum.

Cabri, L.J. (2004) New developments in process mineralogy of platinum-bearing ores. *Proceedings of the Canadian Mineral Processors, 36th annual meeting*, pp. 189–198.

Challis, G.A. and Long, J.V.P. (1964) Wairauite – a new cobalt-iron mineral. *Mineralogical Magazine*, **33**, 942–948.

Ellis, W.C. and Greiner, E.S. (1941) Equilibrium relations in the solid state of the iron-cobalt system. *Transactions of the American Society of Metals*, **29**, 415–434.

Irvine, T.N. (1992) Emplacement of the Skaergaard Intrusion. *Carnegie Institution of Washington Year Book*, **91**, 91–96.

Irvine, T.N., Andersen, J.C.Ø and Brooks, X.X. (2001) Excursion guide to the Skaergaard intrusion, Kangerdlugssuaq area, east Greenland. *International Geological Correlation Project*, **1**.

Jambor, J.L. and Grew, E.S. (1990) New mineral names. *American Mineralogist*, **75**, 240–246.

Karup-Møller, S. and Makovicky, E. (1999) The phase system Cu-Pd-S at 900 degrees, 725 degrees, 550 degrees, and 400 degrees C. *Neues Jahrbuch für Mineralogie, Monatshefte*, **1999**, 551–567.

Kravchenko, T.A. and Kolonin, G.R. (1996) Dependences of stable forms of platinum and palladium on the composition of copper-containing sulphide associates (by experimental data). *Experiment in Geosciences*, **5**, 53–54.

Komppa, U. (1998) *Oxide, sulphide and platinum mineralogy of the South Kawishiwi and Partridge River Intrusions of the Duluth Layered Intrusion Complex, Minnesota, U.S.A.* MSc thesis, Department of Geosciences, University of Oulu, Finland, 104 pp. (in Finnish).

Kwitko, R., Cabral, A.R., Lehmann, B., Laflamme, J.H.G., Cabri, L.J., Criddle, A.J. and Galbiatti, H.F. (2002) Hongshiite, PtCu, from itabirite-hosted Au-Pd-Pt mineralization (Jacutinga), Itabira district, Minas Gerais, Brazil. *The Canadian Mineralogist*, **40**, 711–723.

Makovicky, E. (2002) Ternary and quaternary phase systems with PGE. Pp. 131–175 in: *The Geology, Geochemistry, Mineralogy, Mineral Beneficiation of the Platinum-Group Elements* (L.J. Cabri, editor). Special Volume **54**, Canadian Institute of Mining, Metallurgy and Petroleum.

Nielsen, T.D.F., Rasmussen, H., Rudashevsky, N.S., Kretser, Yu.L. and Rudashevsky, V.N. (2003) *PGE and sulphide phases of the precious metal mineralization of the Skaergaard intrusion. Part 2: sample 90-24 1057*. Geological Survey of Denmark and Greenland report 2003/48, 20 pp.

Nolze, G. and Kraus, W. (1998) *Powdercell*, *v*. 2.3. Federal Institute for Materials Research and Testing, Berlin, Germany.

Nowotny, H. and Winkels, A. (1939) Zur Überstruktur von β-Messing. *Zeitschrift für Physik*, **114**, 455–458.

Power, M.R., Pirrie, D., Anderson, J.C.Ø and Butcher, A.R. (2000) Stratigraphical distribution of platinum-group minerals in the Eastern Layered Series, Rum, Scotland. *Mineralium Deposita*, **35**, 762–775.

Rudashevsky, N.S., Garuti, G., Andersen, J.C.Ø., Kretser, Y.L., Rudashevsky, V.N. and Zaccarini, F. (2002) Separation of accessory minerals from rocks and ores by hydroseparation (HS) technology: method and application to CHR-2 chromitite, Niquelândia, Brazil. *Transactions, Institution of Mining and Metallurgy/ Proceedings Australasian Institute Mining Metallurgy, Section B: Applied Earth Science*, **111**, 87–94.

Rudashevsky, N.S., Lupal, S.D. and Rudashevsky, V.N. (2001) The hydraulic classifier. Russia patent N 2165300. *Patent Cooperation Treaty PCT/ RU01/ 00123 (Moscow: 20 April 2001; 10 May 2001)* (in Russian and English).

Saini-Eidukat, B., Weiblen, P.W., Bitsianes, G. and Glascock, M.D. (1990) Contrasts between platinum group element contents and biotite compositions of Duluth Complex troctolitic and anorthositic series rocks. *Mineralogy and Petrology*, **42**, 121–140.

Stanley, C.J., Criddle, A.J., Förster, H.-J. and Roberts, A.C. (2002) Tischendorfite, $Pd_8Hg_3Se_9$, a new mineral species from Tilkerode, Harz Mountains, Germany. *The Canadian Mineralogist*, **40**, 739–745.

Wang, K. (1986) Zhanghengite – a new mineral. *Acta Mineralogica Sinica*, **6**, 220–223.

Yu, Z. (2001) New data on daomanite and hongshiite. *Acta Geologica Sinica*, **75**, 458–465.

[*Manuscript received 7 April 2004: revised 6 July 2004*]